Three-dimensional, Flexible Graphene Bioelectronics*

SungGyu Chun†, Jonghyun Choi†, Ali Ashraf, SungWoo Nam, *Member, IEEE*

***Abstract* — We report 3-dimensional (3D) graphene-based biosensors fabricated via 3D transfer of monolithic graphene-graphite structures. This mechanically flexible all-carbon structure is a prospective candidate for intimate 3D interfacing with biological systems. Monolithic graphene-graphite structures were synthesized using low pressure chemical vapor deposition (LPCVD) process relying on the heterostructured metal catalyst layers. Nonplanar substrates and wet-transfer method were used with a thin Au film as a transfer layer to achieve the 3D graphene structure. Instead of the typical wet-etching method, vapor-phase etching was performed to minimize the delamination of the graphene while removing the transfer layer. We believe that the monolithic graphene-graphite synthesis combined with the conformal 3D transfer will pave the way for the 3D conformal sensing capability as well as the intracellular recording of living cells in the future.**

I. Introduction

Graphene is a one-atom thick sheet of carbon atoms packed in a sp^2-bonded atomic scale hexagonal lattice [1]. Graphene has been drawing significant attention owing to its unique physical properties such as extremely high carrier mobility, mechanical stability and flexibility, and thermal conductivity [2-4]. Superb electromechanical properties of graphene, where the electrical properties remain almost constant even when applying more than 20% of elastic deformation, provide a promising platform material to realize flexible and implantable 3-dimensional (3D) biosensor devices [5-7].

Several groups have reported electrical measurements from cells/tissues interfaced to graphene-based field-effect transistors (Gra-FETs) [8-14]. Typical ambipolar behavior of Gra-FETs with high signal-to-noise ratio was shown, demonstrating the potential advantage over conventional nano-FET sensors [10]. Selective interaction/response of Gra-FETs has been reported, by functionalizing the surface of graphene [13]. These graphene based devices, however, are typically planar structures and the electrode materials consist of metal, which present significant challenges for 3D flexible bioelectronics.

*This work was supported by the Air Force Office of Scientific Research/Asian Office of Aerospace Research Development (AFOSR/AOARD) Nano Bio Info Technology (NBIT) Phase III Program (AOARD-13-4125), American Chemical Society (ACS) Petroleum Research Fund (53270-DNI10), and by the University of Illinois, Urbana-Champaign (UIUC) startup funding.

†S. Chun and J. Choi contributed equally to this work.

S. Chun, J. Choi and A. Ashraf are with the Department of Mechanical Science and Engineering, University of Illinois, Urbana-Champaign, IL 61801 USA.

Prof. S. Nam is with the Department of Mechanical Science and Engineering and Materials Science and Engineering, University of Illinois, Urbana-Champaign, IL 61801 USA (e-mail: swnam@illinois.edu).

Here we report a single-step synthesis of graphene-graphite based electronics and conformal/uniform transfer onto nonplanar 3D substrates, to realize 3D interfacing of graphene FETs to biological systems. Such capability to synthesize monolithic graphene-graphite integrated electronics and further to integrate with 3D substrates will pave the way for integrated bio-electronics which conform to the dimensionality and mechanical properties of target cells/tissues [6-7].

II. Monolithic Synthesis and Characterization of Flexible Graphene-Graphite Structures

We demonstrate the controlled synthesis of graphene and graphite by utilizing differences in carbon solubility of heterogeneous catalyst metals during chemical vapor deposition (CVD) synthesis [6]. By patterning different catalyst metals on designated areas, graphene with varying thickness can be grown on localized areas. Thick multilayer graphene (i.e., graphite) is grown by segregation and precipitation of the dissolved carbon on the surface of catalyst metals, such as Ni or Co [6, 15, 16]. Thin or single layer graphene is synthesized by adsorption of carbon on the catalyst Cu surface, which only has negligible carbon solubility (<0.0001 at.% at 1000 °C) [6, 17]. Figure 1 shows the optical image of localized graphene and graphite layers by patterning heterogeneous metal letters.

Figure 1. Synthetic control of graphene layers. Optical microscope images of graphene with different number of layers. Letters on top are composed of thinner graphite and letters on bottom are composed of thicker graphite. Background is compsed of bi- to tri-layer garphene on a 285 nm thick SiO_2/Si substrate.

The electrical properties of graphene can be controlled by changing the number of layers. It is known that the conductivity or sheet resistance of multilayer graphene can be modulated by more than two orders of magnitude by performing controlled synthesis of graphene multilayers on different metal catalysts [6].

Even with the same catalyst metal, the thickness of graphite could be controlled by modulating the thickness of the catalyst layer.

Figure 2. Optical microscope image of graphene with different number of layers. Consonant letters are composed of thinner graphite and vowel letters are composed of thicker graphite. Background is compsed of bi- to tri-layer garphene on a 285 nm thick SiO_2/Si substreate.

Figure 2 shows the optical image of graphite letters and graphene background synthesized on different catalyst metals. Vowels (i.e. E's) were patterned with thicker Co (750 nm) on Cu background (700 nm), while consonants (i.e. C, H, M and S) were patterned with thinner Co (200 nm). The color contrast between vowels and consonants shows the difference in thickness of synthesized graphite.

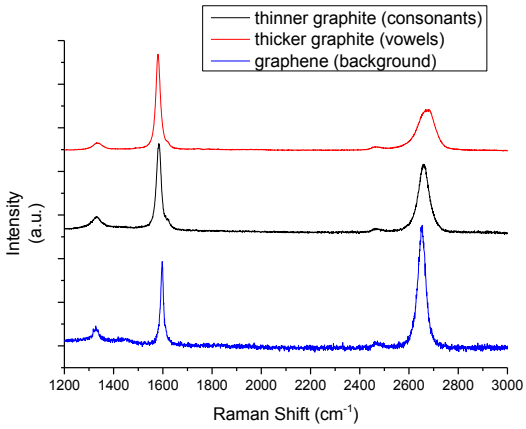

Figure 3. Raman spectra of graphite and graphene with different thickness: red (thicker graphite; vowels), black (thinner graphite; consonants), and blue (bilayer graphene; background).

We also performed Raman characterizations to demonstrate thickness control (Figure 3). Raman spectra from these three different graphite or graphene regions exhibited the three characteristic bands of graphene and graphite: (1) D band centered at ~1,350cm^{-1}, (2) G band centered at 1,590cm^{-1}, and (3) 2D band centered at ~2,690cm^{-1} [6]. The background graphene shows a smaller G band intensity compared to the 2D band intensity (2D/G~1.6), indicating bi- or tri-layer graphene. The graphite on vowel regions shows a much lower 2D band intensity compared to that on consonant regions. This low 2D to G ratio, non-symmetric tendencies, and a slight blue-shift due to interlayer binding prove that the graphite on vowel regions represents much thicker graphite than that on consonant regions.

III. Electrical Characterization of Graphene Bioelectronics

We carried out the device fabrication and electrical measurement of graphene FETs. Figure 4 shows the fabricated graphene FET with Au metal contacts. Nine individual graphene FET channels were patterned, followed by the Au contacts, with standard photolithography and thermal evaporation.

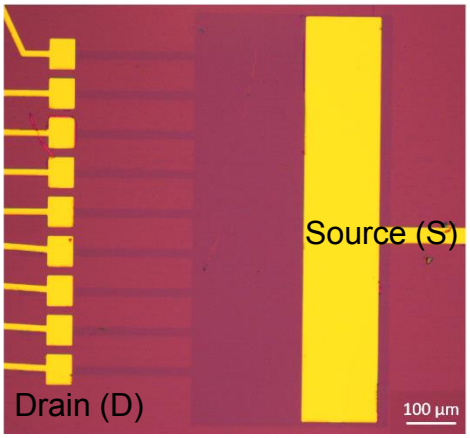

Figure 4. Optical microscope image of fabricated graphene FET device array.

The electrical characterization of graphene FET is shown in Figure 5. The I_{ds}-V_{ds} characteristics of graphene FET shows the linear behavior at room temperature, which indicates Ohmic contact behavior.

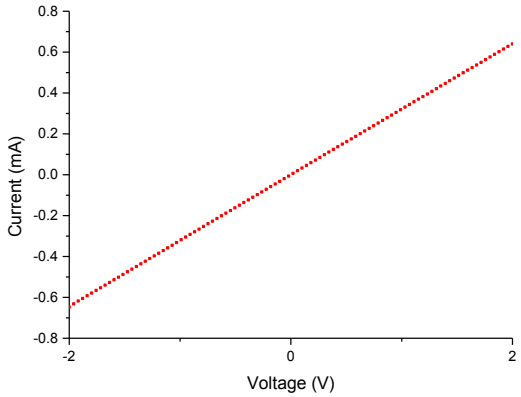

Figure 5. I_{ds}-V_{ds} of the graphene FET devices with Au contacts.

We further performed S/D current (I_{ds}) versus back-gate bias (V_{gs}) characterization of the graphene FET structure at room temperature (Figure 6). The result demonstrates that the fabricated device showed p-type behavior within a gate voltage (-100 V ~ 100 V), possibly due to adsorbates in air [18].

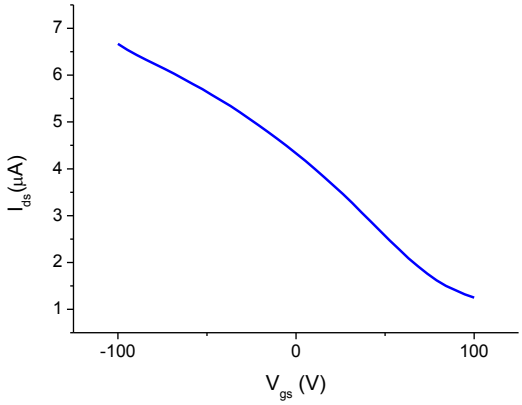

Figure 6. I_{ds}-V_{gs} of the graphene FET devices with Au contacts.

IV. 3D Transfer of Graphene Devices for 3D Bio-interfacing

A. 3D Conformal Large Area Graphene Transfer

Due to its mechanical flexibility and robustness, graphene can be transferred onto various nonplanar substrates and form a conformal 3D structure. Figure 7 illustrates the fabrication procedure for transfer of graphene onto pyramid-shaped substrate. Pyramid arrays of polydimethylsiloxane (PMDS), which exhibits superior biocompatibility, were fabricated and used as substrate material [19]. A thin Au layer was used as a transfer/sacrificial material for the solution transfer method; the Au layer provides ductility that is crucial for the conformal transfer, which is challenging for conventional poly(methyl methacrylate) (PMMA) layers that are relatively brittle.

To remove the Au layer after the transfer, vapor phase etching was performed in a sealed chamber at room temperature. Compared to typical wet etching methods, this method minimizes the damage or delamination of graphene during the etching process. Figure 8 shows the optical microscope and scanning electron microscope (SEM) images of the graphene transferred onto the pyramid arrays. Graphene was uniformly covered over a wide area and it was conformal with the underlying 3D features without significant suspensions/damages.

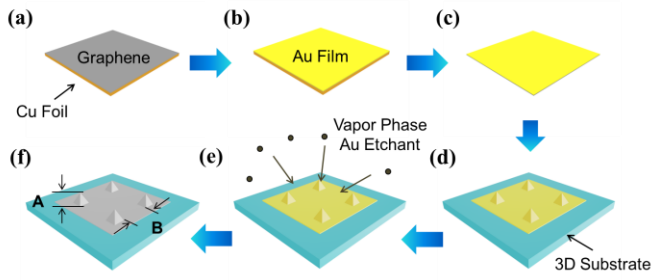

Figure 7. Schematic illustration of 3D graphene transfer. (a) Graphene synthesis based on CVD on a 25 um-thick mechanically polished Cu foil. (b) Thin Au film deposition (30 nm) onto graphene/Cu. (c) Etching the Cu catalyst layer. (d) Solution transfer onto various nonplanar substrates. (e) Removal of the Au sacrificial layer is based on vapor-phase etching. (f) Graphene on 3D substrates. A and B indicate the height and the distance between the shapes, respectively.

B. Raman Characterization of 3D Graphene

To further demonstrate that graphene was not damaged with respect to the 3D features, Raman characterizations were carried out (Figure 9). I_{2D}/I_G ratios of 2.86 and 2.72 for 3D and planar graphene, respectively, without significant D band, demonstrate that graphene was successfully transferred over a large area. The Raman shift of 2D bands as well as the full width at half maximum (FWHM) were also analyzed. For 3D graphene, dispersive (broader) and blue-shifted 2D bands were observed compared to planar graphene.

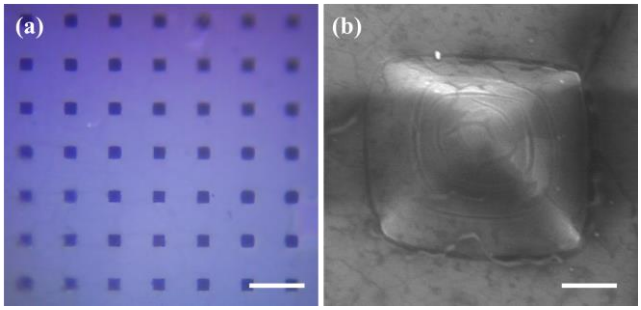

Figure 8. (a) Optical microscope image of monolayer graphene transferred onto PDMS pyramids array. Scale bar: 10 µm. (b) 30º tilted SEM image of a single PDMS pyramid with the graphene. Scale bar: 1 µm.

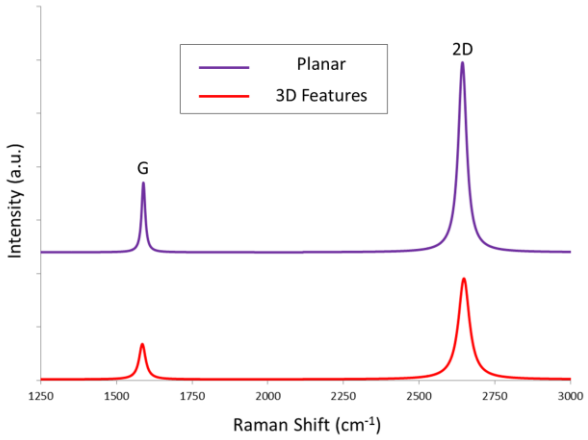

Figure 9. Raman spectra demonstrating graphene existing on 3D features and nearby planar area. The wavelength of the excitation laser was 633 nm. The Raman spectrum from the underlying PDMS was subtracted to clearly visualize only 2D (2,632–2,778 cm^{-1}) and G (1,537–1,624 cm^{-1}) bands.

V. Discussion and Conclusion

We have demonstrated monolithic synthesis of mechanically flexible graphene/graphite structures with controlled thickness of graphene layers. In addition, these graphene structures were fabricated into arrays of FETs. Furthermore, we have demonstrated conformal 3D transfer of free-standing graphene layers for the first time for the integration of graphene devices onto 3D structures. We believe that the monolithic synthesis of graphene-graphite and 3D integration provides unique capabilities to form conformal and flexible 3D interfaces with biological systems. Future studies will be focused on 3D intra- and extracellular electrophysiology of electrogenic cells/tissues based on developed structures and devices.

References

[1] A. K. Geim, "Graphene: status and prospects," *Science*, vol. 324, pp. 1530-1534, Jun. 2009.

[2] A. K. Geim, K. S. Novoselov, "The rise of graphene," *Nature Mater.*, vol. 6, pp. 183-191, Mar. 2007.

[3] A. H. Castro Neto *et al*., "The electronic properties of graphene," *Rev. Mod. Phys*, vol. 81, pp. 109, Jan. 2009.

[4] F. Schwierz, "Graphene Transistors," *Nature Nanotech.,* vol. 5, pp. 487-496, May. 2010.

[5] K. S. Kim *et al.*, "Large-scale pattern growth of graphene films for stretchable transparent electrodes," *Nature*, vol. 457, pp. 706-710, Feb. 2009.
[6] J.-U. Park, S. Nam, M.-S. Lee and C. M. Lieber, "Synthesis of monolithic graphene-graphite integrated electronics," *Nature Mater*., vol. 11, pp. 120-125, Feb. 2012.
[7] S. Nam, S. Chun, and J. Choi, "All-carbon graphene bioelectronics," *35th Annu. Int. Conf. IEEE Eng. Med. Biol. Soc.*, Osaka, Japan, 2013, pp. 5654-5657.
[8] P. K. Ang *et al.*, "A Bioelectronic Platform Using a Graphene−Lipid Bilayer Interface," *ACS Nano*, vol. 4, pp. 7387-7394, Nov. 2010.
[9] R. Daly *et al*., "Cell Proliferation Tracking Using Graphene Sensor Arrays," *J. Sensors*, vol. 2012, http://dx.doi.org/10.1155/2012/219485, Aug. 2011.
[10] T. Cohen-Karni *et al.*, "Graphene and Nanowire Transistors for Cellular Interfaces and Electrical Recording," *Nano Lett.,* vol. 10, pp. 1098-1102, Feb. 2010.
[11] P. Nguyen, V. Berry, "Graphene Interfaced with Biological Cells: Opportunities and Challenges," *J. Phys. Chem. Lett.*, vol. 3, pp. 1024-1029, Mar. 2012.
[12] L. H. Hess *et al.*, "Graphene Transistor Arrays for Recording Action Potentials from Electrogenic Cells," *Adv. Mater.*, vol. 23, pp. 5045-5049, Nov. 2011.
[13] J. H. An *et al.*, "High-Performance Flexible Graphene Aptasensor for Mercury Detection in Mussels," *ACS Nano*, vol. 7, pp. 10563-10571, Nov. 2013.
[14] J. Choi *et al.*, "Graphene bioelectronics," *Biomed. Eng. Lett.,* vol. 3, pp. 201-208, Dec. 2013.
[15] S. Bae *et al*., "Roll-to-roll production of 30 inch graphene films for transparent electrodes," *Nature Nanotech*., vol. 5, pp. 574-578, Aug. 2010.
[16] A. Reina *et al*., "Large area, few-layer graphene films on arbitrary substrates by chemical vapor deposition," *Nano Lett*., vol. 9, pp. 30-35, Dec. 2008.
[17] X. Li, W. Cai, L. Colombo and R. S. Ruoff, "Evolution of graphene growth on Ni and Cu by carbon isotope labeling," *Nano Lett*., vol. 9, pp. 4268-4272, Aug. 2009
[18] B. Guo et al., "Controllable N-Doping of Graphene," *Nano Lett.*, vol. 10, pp. 4975-4980, Oct. 2010.
[19] D. S. Lee *et al.*, "Biocompatibility of a PDMS-coated micro-device: Bladder volume monitoring sensor," *Chinese J. Polymer. Science*, vol. 30, pp. 242-249, Mar. 2012.